Photochemistry of the tris(2,2'-bipyridine)ruthenium(II)-peroxydisulfate system in aqueous and mixed acetonitrile-water solutions. Evidence for a long-lived photoexcited ion pair

Henry S. White, William G. Becker, and Allen J. Bard

J. Phys. Chem., **1984**, 88 (9), 1840-1846• DOI: 10.1021/j150653a033 • Publication Date (Web): 01 May 2002

vacuum UV photolysis of CH_2CH_2 at 1849 Å. The ratio between molecular and diatom elimination of H_2 vs. H ejections was reported as 0.86:0.14, whereas in the present work the corresponding ratio is 0.87:0.13.

On the other hand, Wijnen and co-workers[30] observed in their studies on CH_2CHCl photolysis that at $\lambda > 2000$ Å the main route of CH_2CHCl^* decay was via Cl ejection rather than HCl molecular elimination. Most probably this preference of atom ejection is due to the much weaker C–Cl bond. However, at shorter wavelengths $\lambda \sim 1470$ Å, the molecular elimination began to be favored as observed in the present study.

Vacuum UV Photochemistry of CH_2CF_2. By analogy with the previous discussion on CH_2CHF photochemistry, the decay of CH_2CF_2 can be expected to follow the sequence:

$$CH_2CF_2^* \rightarrow HF^\dagger + HCCF \quad (2)$$

$$CH_2CF_2^* \rightarrow F + CH_2CF^\dagger \quad (14)$$

$$F + CH_2CF_2 \rightarrow [C_2H_2F_3]^\dagger \quad (15)$$

$$[C_2H_2F_3]^\dagger \rightarrow CHFCF_2 + H \quad (16)$$

$$[C_2H_2F_3]^\dagger + He \rightarrow [C_2H_2F_3] + He \quad (17)$$

$$[C_2H_2F_3] + CH_2CF_2 \rightarrow CH_2FCF_2CH_2CF_2, \text{ etc.} \quad (18)$$

$$CH_2CF^\dagger + CH_2CF_2 \rightarrow CH_2CHF + CF_2CH \quad (19)$$

$$[C_2H_2F_3]^\dagger \rightarrow \textit{trans}\text{-CHFCHF } (\textit{cis}\text{-CHFCHF}) + F \quad (20)$$

$$CH_2CF_2^* \rightarrow \textit{trans}\text{-CHFCHF } (\textit{cis}\text{-CHFCHF}). \quad (21)$$

(30) P. Ausloos, R. E. Rebbert, and M. H. J. Wijnen, *J. Res. Natl. Bur. Stand., Sect. A*, **77**, 243 (1973).

All stable products from these reactions were observed in the GC. Like $[C_2H_3F_2]^\dagger$, $[C_2H_2F_3]^\dagger$ is expected to exhibit a He stabilization vs. decomposition (reactions 16 and 17). Although *trans*-CHFCHF was also observed in the CH_2CHF photodecomposition, it was a minor product relative to its concentration in the CH_2CF_2 photodecomposition. Quantitative studies like those for CH_2CHF were not conducted on CH_2CF_2 samples, preventing one from estimating primary branching ratios.

Conclusions

The primary route of CH_2CHF and CH_2CF_2 decay upon exposure to broad-band vacuum UV radiation above 1550 Å is direct α–β photoelimination of molecular HF. The photoelimination is sufficiently exothermic to produce rotationally excited HF up to $v = 1$, $J = 31$ as observed in the rotational laser experiments. At most, the F abstraction of H could result in 5% of the observed HF. Excluding single H atom ejection, which could not be identified in the present experimental design, the primary branching ratios for the decay of the photoexcited CH_2CHF are as follows: HF molecular elimination, 0.82 ± 0.05; F atom ejection, 0.13 ± 0.04; HH molecular or diatom elimination, 0.05 ± 0.04. Pressure studies of the CH_2CHF decay indicate that a difluoroethyl radical ejects an H atom and forms the 1,1-difluoroethene.

Acknowledgment. We gratefully acknowledge research support from the Air Force Office of Scientific Research under Grant no. 78-3535.

Registry No. CH_2CHF, 75-02-5; CH_2CF_2, 75-37-6; CH_2CH_2, 74-85-1; HCCF, 2713-09-9; HCCH, 74-86-2; *trans*-CHFCHF, 1630-78-0; CF_2CHF, 359-11-5; *cis*-CHFCHF, 1630-77-9; CF_2CF_2, 116-14-3; He, 7440-59-7; Ne, 7440-01-9; Ar, 7440-37-1; Kr, 7439-90-9; CO, 630-08-0; NO, 10102-43-9.

Photochemistry of the Tris(2,2′-bipyridine)ruthenium(II)–Peroxydisulfate System in Aqueous and Mixed Acetonitrile–Water Solutions. Evidence for a Long-Lived Photoexcited Ion Pair

Henry S. White, William G. Becker, and Allen J. Bard*

Department of Chemistry, The University of Texas, Austin, Texas 78712 *(Received: May 26, 1983)*

The photooxidation of $Ru(bpy)_3^{2+}$ (bpy = 2,2′-bipyridine) by peroxydisulfate, $S_2O_8^{2-}$, was investigated by steady-state luminescence quenching and emission lifetime techniques in aqueous and mixed CH_3CN–H_2O solutions. The resulting Stern–Volmer plots showed downward curvature for data obtained from solutions of increasing ionic strength, S-shaped curves for data obtained in solutions of low but constant ionic strength, and linear plots from solutions of high ionic strength. The results are consistent with the formation of a ground-state ion pair $[Ru(bpy)_3^{2+}\cdot S_2O_8^{2-}]$. The lifetime of the photoexcited ion pair–ion pair association constant and oxidative rate constant are reported for aqueous and several CH_3CN–H_2O solutions (up to 50% CH_3CN v/v). The lifetime of the photoexcited ion pair $[Ru(bpy)_3^{2+}\cdot S_2O_8^{2-}]^*$ is unusually long, ranging from 0.11 μs in H_2O to 0.53 μs in 50% CH_3CN.

Introduction

The reaction of the excited state of $Ru(bpy)_3^{2+}$ (bpy = bipyridine) with peroxydisulfate, $S_2O_8^{2-}$, to produce the Ru(III) species, has been investigated recently in connection with the design of photoelectrochemical cells[1] and electrogenerated chemiluminescent systems.[2,3] Although Irvine first noted the catalytic effect of sunlight upon the $Ru(bpy)_3^{2+}$–$S_2O_8^{2-}$ reaction,[4] the mechanism and quantum efficiency were only recently established by Bolletta and co-workers.[5]

$$2Ru(bpy)_3^{2+} + S_2O_8^{2-} \xrightarrow{h\nu} 2Ru(bpy)_3^{3+} + 2SO_4^{2-} \quad (1)$$

Because the overall quantum efficiency (i.e., $Ru(bpy)_3^{3+}$ produced/photon absorbed) as shown in eq 1 is 2, the following photoinduced oxidation scheme has been proposed:

(1) Neumann-Spallart, M.; Kalyanasundaram, K.; Grätzel, C.; Grätzel, M. *Helv. Chim. Acta* **1980**, *63*, 1111.
(2) White, H. S.; Bard, A. J. *J. Am. Chem. Soc.* **1982**, *104*, 6891.
(3) Bolletta, F.; Ciano, M.; Balzani, V.; Serpone, N. *Inorg. Chim. Acta* **1982**, *62*, 207.
(4) Irvine, D. H. *J. Am. Chem. Soc.* **1959**, *81*, 2977.
(5) Bolletta, F.; Juris, A.; Maestri, M.; Sandrini, D. *Inorg. Chim. Acta* **1980**, *44*, L175.

0022-3654/84/2088-1840$01.50/0

$$Ru(bpy)_3^{2+} \xrightarrow{h\nu} Ru(bpy)_3^{2+*} \quad (2)$$

$$Ru(bpy)_3^{2+*} + S_2O_8^{2-} \xrightarrow{k_q} Ru(bpy)_3^{3+} + SO_4^{-}\cdot + SO_4^{2-} \quad (3)$$

$$Ru(bpy)_3^{2+} + SO_4^{-}\cdot \xrightarrow{\text{fast}} Ru(bpy)_3^{3+} + SO_4^{2-} \quad (4)$$

The strongly oxidizing intermediate, $SO_4^{-}\cdot$, produced during the rate-determining step, reaction 3, generates a second Ru(III) species through a following facile ground-state reaction (eq 4).

Reports from our laboratory[2] and that of Bolletta and co-workers[3] have described electrogenerated chemiluminescent (ecl) and chemiluminescent (cl) systems that involve the oxidation of $Ru(bpy)_3^{2+}$ by $S_2O_8^{2-}$. The efficiency and light output of this system are limited, in part, by the quenching of $Ru(bpy)_3^{2+*}$ by $S_2O_8^{2-}$ (eq 3.)[2] The bimolecular quenching rate, k_q, and thus the ecl and cl efficiencies depend strongly upon the solvent employed and the $S_2O_8^{2-}$ concentration. For example, while k_q approaches diffusion-controlled rates ($>10^9$ M^{-1} s^{-1}) in aqueous solutions,[1] it is several orders of magnitude slower in dimethyl sulfoxide ($<10^7$ M^{-1} s^{-1}),[6] a difference not obviously attributable to a change in solvent viscosity or dielectric constant. Previously published luminescence quenching and excited-state lifetime measurements of the $Ru(bpy)_3^{2+}$–$S_2O_8^{2-}$ system[1,5] have indicated that the initial photoinduced electron transfer occurs in a collision between excited $Ru(bpy)_3^{2+*}$ and $S_2O_8^{2-}$. Plots of τ^0/τ vs. $[S_2O_8^{2-}]$ (where τ and τ^0 represent the observed lifetime of $Ru(bpy)_3^{2+*}$ in the presence and absence of $S_2O_8^{2-}$, respectively) exhibit normal Stern–Volmer behavior (eq 5). For example, in aqueous solutions of constant

$$\tau^0/\tau = 1 + k_q\,\tau^0[S_2O_8^{2-}] \quad (5)$$

ionic strength (0.1 M acetate), Grätzel and co-workers found the photooxidation rate constant to be nearly diffusion controlled (8×10^8 M^{-1} s^{-1}) and independent of $S_2O_8^{2-}$ concentration.[1] However, in related studies of the ground-state oxidation of *o*-phenanthroline and bipyridine complexes of iron(II) by $S_2O_8^{2-}$, Brubaker and Raman demonstrated that electron transfer proceeded via a precursor ion pair between the 2+ and 2– reactants.[7]

$$Fe(bpy)_3^{2+} + S_2O_8^{2-} \overset{K_{eq}}{\rightleftharpoons} (Fe(bpy)_3^{2+}\text{–}S_2O_8^{2-}) \quad (6)$$

$$(Fe(bpy)_3^{2+}\text{–}S_2O_8^{2-}) \rightarrow Fe(bpy)_3^{3+} + SO_4^{2-} + SO_4^{-}\cdot \quad (7)$$

Detailed kinetic studies of this reaction and others provided values of the association constant, K_{eq}. In view of the structural and charge similarities between $Ru(bpy)_3^{2+}$ and $Fe(bpy)_3^{2+}$, ion-pair formation could also play a role in the photochemical kinetics of the $Ru(bpy)_3^{2+}$–$S_2O_8^{2-}$ system. In this paper we report the results of luminescence and lifetime measurements of the $Ru(bpy)_3^{2+}$–$S_2O_8^{2-}$ system in aqueous and mixed H_2O–CH_3CN solutions. We found that, in a mechanism similar to the ground-state oxidation of Fe(II) complexes, the photooxidation of $Ru(bpy)_3^{2+}$ occurs predominantly through the ground-state precursor complex, $[Ru(bpy)_3^{2+}\cdot S_2O_8^{2-}]$, in solutions of relatively low ionic strength and that this mechanism accounts for the large difference in quenching rate between aqueous and CH_3CN solutions.

Experimental Section

Chemicals. $Ru(bpy)_3(PF_6)_2$ was prepared and purified as previously reported.[2] Ammonium peroxydisulfate (MCB or Allied Chemical) was recrystallized from EtOH–water at room temperature to remove contaminant sulfate. Even freshly opened bottles of $(NH_4)_2S_2O_8$ were found to contain a significant fraction (>10%) of impurity. Potassium ferrocyanide (MCB) was recrystallized from EtOH–water. Ammonium sulfate (MCB) was used without further purification. Triply distilled water and reagent-grade acetonitrile (MCB) were used throughout.

Photochemical Apparatus and Procedure. Emission spectra were obtained with an Aminco-Bowman spectrophotofluorimeter adapted to a Princeton Applied Research Model 1215-1216 optical multichannel analyzer. An ISA holographic grating (147 lines/mm) reconstructed the emission spectra on the target face of a Model 1254 SIT Vidicon detector. A 150-W xenon lamp was employed as the excitation source. A 1-cm^2 fluorescence cell and 1-mm excitation and emission slits were used in all steady-state luminescence measurements.

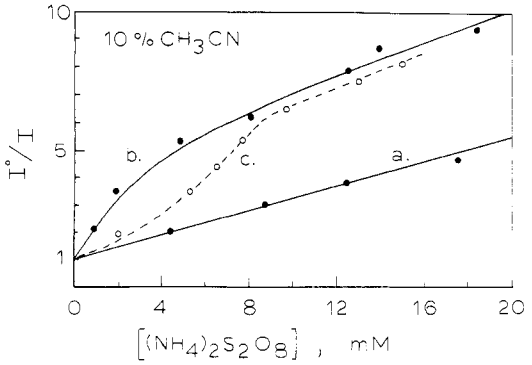

Figure 1. Stern–Volmer plot for 10% CH_3CN (by volume) solutions containing (a) 0.2 M $(NH_4)_2SO_4$, (b) no additional electrolyte, and (c) a total concentration of $(NH_4)_2SO_4$ and $(NH_4)_2S_2O_8$ equal to 15 mM. All solutions contained ~30 μM $Ru(bpy)_3(PF_6)_2$ and were purged with N_2. The solid line drawn through curve b was calculated from eq 19 (see text) with K_{eq} = 1300 M^{-1}, $k_q = 4.3 \times 10^8$ M^{-1} s^{-1}, $k_q' = 4.2 \times 10^8$ M^{-1} s^{-1}, τ^0 = 0.64 μs, and τ' = 0.13 μs.

Lifetime Measurements. Solutions containing $Ru(bpy)_3^{2+}$ were excited with a 355-nm pulse (275 mJ, 10 ns fwhm), the third harmonic of a Q-switched Nd:YAG laser (Quantrel YG 481). The transient emissions were monitered at 650 nm and digitized with a Biomation 8100 digitizer. The digitized transient decay was analyzed with either a DEC PDP 11/34 or PDP 11/70 computer.

$Ru(bpy)_3^{2+}$ and $S_2O_8^{2-}$ solutions were prepared and stored under darkroom conditions immediately before each experiment to prevent possible changes in concentration due to the photoreaction (eq 1). Precautions were taken to prevent changes in the reactant concentration during each experiment by avoiding long irradiation exposures. In the steady-state quenching experiments the acquisition time necessary to obtain an emission spectrum was approximately 10 s, during which time the solution was exposed to low-level monochromatic light. Repetitive spectra indicated that the emission intensity decreased by 2% during this period. Similarly, only the initial luminescence intensity–time profiles of freshly prepared solutions were used in analyzing lifetime measurements.

The $Ru(bpy)_3^{2+}$ concentration employed in quenching measurements varied from 3 to 30 μM, corresponding to an absorbance of 0.04–0.4 (ϵ 14 000 M^{-1} cm^{-1}) with no effect on the resulting Stern–Volmer plots. Excitation at either 450 or 350 nm yielded indistinguishable I^0/I values. All steady-state measurements were made with solutions irradiated at 450 nm.

All solutions were thoroughly purged with prepurified nitrogen that was saturated with the solvent employed. Temperature variation in the steady-state luminescence experiments was accomplished by the apparatus previously described.[8]

Results

Steady-State Luminescence and Lifetime Measurements. Emission from $Ru(bpy)_3^{2+*}$ in aqueous and mixed CH_3CN–H_2O solutions (up to 50% CH_3CN by volume) was quenched by the addition of $S_2O_8^{2-}$ at rates that were investigated by steady-state luminescence and lifetime measurements. Typical Stern–Volmer (SV) plots obtained from measurements in 10% and 40% CH_3CN solutions containing a high concentration of additional electrolyte, 0.2 M $(NH_4)_2SO_4$ (Figures 1a and 2a), yield essentially identical results for both lifetime and luminescence measurements; these suggest a bimolecular process, i.e., plots of I^0/I or τ^0/τ vs. $[S_2O_8^{2-}]$ were linear with a unity intercept (eq 5). Similar results obtained

(6) Seung, S.; White, H. S.; Bard, A. J., The University of Texas at Austin, unpublished results.

(7) Raman, S.; Brubaker, C. H. *J. Inorg. Nucl. Chem.* **1969**, *31*, 1091.

(8) Wallace, W. L.; Bard, A. J. *J. Phys. Chem.* **1979**, *83*, 1350.

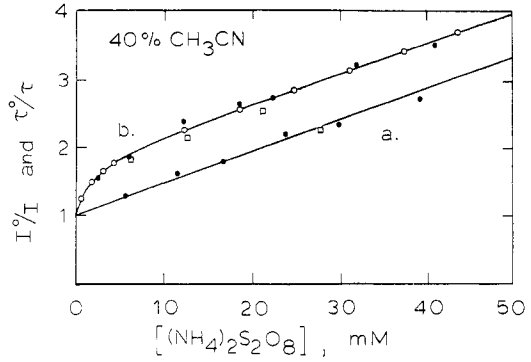

Figure 2. I^0/I (●) and τ^0/τ (□) as a function of $[S_2O_8^{2-}]$ in 40% CH_3CN (by volume) solutions containing (a) 0.2 M $(NH_4)_2SO_4$, and (b) no additional electrolyte. The solid line drawn through the luminescence data in part b was calculated from eq 19 (see text) with $K_{eq} = 650\ M^{-1}$, $k_q = k_q' = 3.4 \times 10^7\ M^{-1}\ s^{-1}$, $\tau^0 = 0.81\ \mu s$, $\tau' = 0.46\ \mu s$. Values of τ^0/τ calculated from eq 22 are denoted by open circles (○). Values used in calculation of τ^0/τ are the same as for the solid line (theoretical I^0/I vs. $[S_2O_8^{2-}]$) described above. All solutions contained ~30 μM $Ru(bpy)_3(PF_6)_2$ and were purged with N_2.

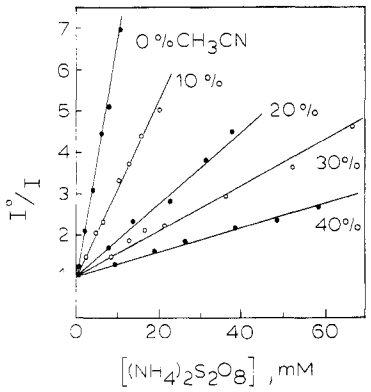

Figure 3. Stern–Volmer plots for solutions containing 0–40% CH_3CN (by volume) and 0.2 M $(NH_4)_2SO_4$. Excitation at 350 nm; emission monitored at 650 nm. All solutions purged with N_2.

in purely aqueous and various mixed CH_3CN–H_2O solutions containing 0.2 M $(NH_4)_2SO_4$ also obeyed eq 5 (Figure 3). The slopes (equal to $k_q\tau^0$) of the SV plots decreased from 1.1×10^9 $M^{-1}\ s^{-1}$ in purely aqueous solutions to $3.4 \times 10^7\ M^{-1}\ s^{-1}$ in solutions containing up to 40% CH_3CN. This strong solvent dependence is discussed below.

Plots of I^0/I (or τ^0/τ) vs. $[S_2O_8^{2-}]$ deviated significantly from normal Stern–Volmer behavior in solutions not containing additional high concentrations of electrolyte. At $S_2O_8^{2-}$ concentrations ≤ 5 mM the SV plots were curved downward, indicating a rapid decrease in $k_q\tau^0$ with increasing $S_2O_8^{2-}$ concentration (Figure 1b and 2b). At $S_2O_8^{2-}$ concentrations ≥ 5–10 mM the SV plots were linear but showed an extrapolated nonunity intercept. Similar results were obtained for all solutions containing 0–50% CH_3CN (Figure 4). The slopes of the linear segments of these curves decreased with increasing amounts of CH_3CN.

Inspection of parts a and b of Figures 1 or 2 reveal an unusual aspect of the SV plots obtained with solutions in the presence and absence of 0.2 M $(NH_4)_2SO_4$. The linear region of the SV plots obtained in solutions without excess electrolyte are, within experimental error, parallel to the linear SV plots obtained in solutions containing 0.2 M $(NH_4)_2SO_4$. A similar identity of limiting slopes was observed for all solutions containing 10–40% CH_3CN. Investigations of solutions with a higher CH_3CN content were not possible because of the low solubility of $(NH_4)_2SO_4$ in CH_3CN. Such downward curvature in SV plots of luminescence and lifetime measurements for systems involving multiple and oppositely charged reactants has been attributed[9] to a decrease in the reactant

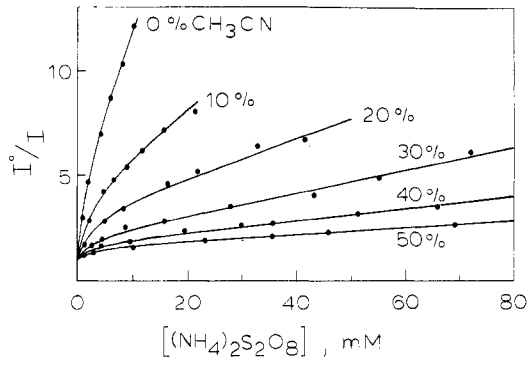

Figure 4. Stern–Volmer plots for solutions containing 0–50% CH_3CN by volume. Excitation at 450 nm; emission monitored at 650 nm. All solutions degassed with N_2.

activities as a result of increasing ionic strength μ.[10,11] This situation can usually be avoided by using solutions of constant ionic strength or by using solutions with a very high concentration of inert electrolyte so that the ionic strength does not vary appreciably as the quencher concentration is changed. Thus, the deviation from linearity in the SV plots obtained from our data in solutions containing no additional electrolyte could be due to such a primary salt (ionic strength) effect; for example, in Figure 1b, μ varies from 0.003 to 0.054 M. However, luminescence quenching experiments obtained in solutions of constant but low ionic strength do not support this explanation. Figure 1c contains the results from such an experiment where the sum of the concentration of $(NH_4)_2SO_4$ and $(NH_4)_2S_2O_8$ is constant and equal to 15 mM ($\mu = 4.5 \times 10^{-2}$ M). The resulting S-shaped SV plot approaches the limiting SV curves obtained with variable ionic strength (Figure 1b) and high ionic strength (Figure 1a, $\mu \cong 0.6$ M) at high and low $S_2O_8^{2-}$ concentrations, respectively. Similar S-shaped curves were obtained for different values of constant ionic strength. The S-shaped curvature of Figure 1c is more suggestive of an association (e.g., ion pairing) between SO_4^{2-} and $S_2O_8^{2-}$ with $Ru(bpy)_3^{2+}$.

Further evidence indicating that primary salt effects do not contribute significantly to the nonlinearity of the SV plots (Figures 1b, 2b, and 4) is obtained from plots of log $(k_q\tau^0)$ vs. $\mu^{1/2}$ (where $k_q\tau^0$ was measured as the slope of the line joining I^0/I at a particular value of $[S_2O_8^{2-}]$ with $I^0/I = 1$ at $[S_2O_8^{2-}] = 0$). For a purely ionic strength effect[10,11] such plots should obey eq 8, where

$$\log (k_q^0\tau^0)/(k_q\tau^0) = 1.02(z_+z_-)\mu^{1/2} \qquad (8)$$

$k_q^0\tau^0$ is the extrapolated quenching constant at $\mu \to 0$. Plots of log $k_q\tau^0$ vs. $\mu^{1/2}$ obtained by varying μ from 0.04 to 0.25 M (by the addition of $(NH_4)_2SO_4$) for a constant $[S_2O_8^{2-}]$ consistently yielded slopes equal to 1–1.5, considerably lower than the predicted value of 4 for 2+ and 2− reactants.

Steady-state luminescence experiments were also performed with $K_4Fe(CN)_6$ as a reductive quencher in 10% CH_3CN solutions, where the ionic strength was allowed to vary as a function of $[K_4Fe(CN)_6]$ from $\mu = 4 \times 10^{-4}$ to 1.2×10^{-3} M. Only a very small departure (downward curvature) from linear SV plots was observed. The quenching rate constant obtained from this experiment was $4.5 \times 10^{10}\ M^{-1}\ s^{-1}$, essentially at the diffusion-controlled value. The small curvature in the SV plot resulting from quenching by $Fe(CN)_6^{4-}$ was negligible as compared to the SV plots shown in Figure 4, again indicating that primary salt effects are not responsible for the unusual behavior observed in the $Ru(bpy)_3^{2+}$–$S_2O_8^{2-}$ system.

Lifetime of $Ru(bpy)_3^{2+*}$ in CH_3CN–H_2O Solutions. The excited-state lifetime of $Ru(bpy)_3^{2+}$, τ^0, in mixed CH_3CN–H_2O solutions was determined from luminescence decay data following

(9) Bolletta, F.; Maestri, M.; Moggi, L. *J. Phys. Chem.* 1973, *77*, 861.

(10) Glasstone, S.; Lewis, D. "Elements of Physical Chemistry"; Van Nostrand: Princeton, NJ, pp 638–9.

(11) Gardiner, W. C., Jr. "Rates and Mechanisms of Chemical Reactions"; W. A. Benjamin: Menlo Park, CA, 1972; pp 158–61.

TABLE I: Results of Kinetic Analysis of the $[Ru(bpy)_3^{2+}\cdot S_2O_8^{2-}]$ System

$[CH_3CN]$, vol %	τ^0,[a] μs	τ',[b] μs	τ^0/τ'[c]	k_q,[d] M^{-1} s^{-1}	k_q',[e] M^{-1} s^{-1}	K_{eq},[f] M^{-1}	$\Delta k_q'$,[g] s^{-1}
0	0.55	0.11	5.0	1.1×10^9	1.3×10^9	1.8×10^3	7.3×10^6
10	0.64	0.13	4.0	4.3×10^8	4.2×10^8	1.3×10^3	4.7×10^6
20	0.71	0.23	3.1	1.3×10^8	1.3×10^8	9.5×10^2	2.9×10^6
30	0.78	0.38	2.05	6.9×10^7	6.8×10^7	7.0×10^2	1.4×10^6
40	0.81	0.46	1.8	3.4×10^7	3.4×10^7	6.5×10^2	9.4×10^5
50	0.82	0.52	1.6		1.8×10^7	5.0×10^2	7.3×10^5

[a] From lifetime measurements in the absence of $S_2O_8^{2-}$. [b] Calculated from intercept of SV plots (τ^0/τ') and τ^0. [c] Intercept of SV plots at low or variable ionic strength. [d] From slope of SV plots in the presence of 0.2 M $(NH_4)_2SO_4$. [e] From slope of SV plots at low or variable ionic strength. [f] Computational best fit to eq 19 (see text). [g] Calculated from eq 24.

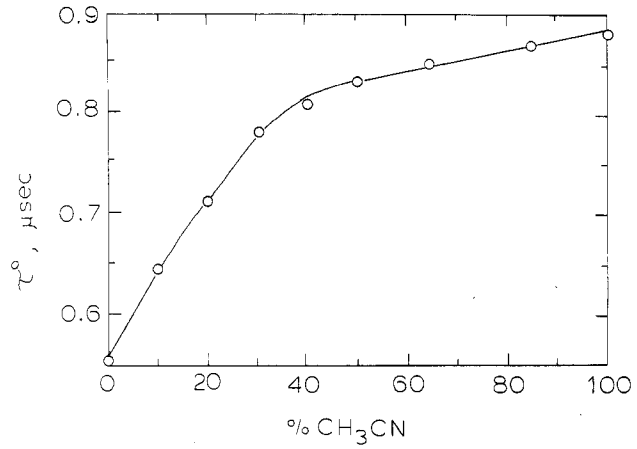

Figure 5. Excited-state lifetime of $Ru(bpy)_3^{2+}$ as a function of CH_3CN content. Same conditions as in Figure 4.

excitation at 355 nm. The counterion present in all solutions was PF_6^-. Emission decay profiles were fitted to a single exponential decay by a least-squares technique. The resulting values of τ^0 are listed in Table I.

The lifetime of $Ru(bpy)_3^{2+*}$ varied from 0.55 μs in purely aqueous solutions to 0.84 μs in solutions containing 50% CH_3CN. An increase in the CH_3CN content of the solution did not result in any further substantial increase in τ^0 (Figure 5). The limiting values of τ^0 in water (0.55 μs) and acetonitrile (0.88 μs) solutions agree well with literature values.[12-15] The virtually constant value of τ^0 in solutions containing greater than 50% CH_3CN probably indicates a preferential solvation of $Ru(bpy)_3^{2+}$ by CH_3CN in CH_3CN–H_2O mixtures. A similar conclusion was reached by Jamieson et al. for $Cr(bpy)_3^{3+}$ in CH_3CN–H_2O solutions from NMR line width measurements.[16]

Analysis of Luminescence Quenching. We believe that the unusual SV plots obtained at low or variable ionic strength are caused by the formation of ground-state ion pairs between $Ru(bpy)_3^{2+}$ and $S_2O_8^{2-}$. Several examples of energy and electron transfer in a photoexcited precursor complex have been reported for organic and inorganic reactants;[17-23] however, the analysis of the resulting lifetime and luminescence measurements of previous studies differs significantly from the one reported here. Consider the general case of ground-state association between the luminescent species, A, and quencher, Q

$$A + Q \overset{K_{eq}}{\rightleftharpoons} (A\cdot Q)$$

(In the present investigation A and Q correspond to $Ru(bpy)_3^{2+}$ and $S_2O_8^{2-}$, respectively.) The fraction of A and (A·Q) of the total analytical concentration of A, C_A, that competes for absorption of light is given by eq 9 and 10.

$$f_A = [A]/C_A = (1 + K_{eq}[Q])^{-1} \quad (9)$$

$$f_{AQ} = [(A\cdot Q)]/C_A = K_{eq}[Q](1 + K_{eq}[Q])^{-1} \quad (10)$$

where $C_A = [A] + [(A\cdot Q)]$. The emission intensity, I, is then

$$I = C_A(f_A\phi_A\epsilon_A + f_{AQ}\phi_{AQ}\epsilon_{AQ}) \quad (11a)$$

$$I^0 = C_A\phi_A{}^0\epsilon_A \quad (11b)$$

where ϕ represents the luminescence quantum yields and ϵ represents the molar absorptivities of A and (A·Q). From eq 9–11 and with the luminescence intensity in the absence of quencher defined as I^0, the general expression for quenching involving ground-state complexation is obtained:

$$I^0/I = \epsilon_A\phi_A{}^0(1 + K_{eq}[Q]/(\phi_A\epsilon_A + K_{eq}[Q]\phi_{AQ}\epsilon_{AQ})) \quad (12)$$

The plots of I^0/I vs. [Q] depend on the values of K_{eq}, ϵ, and ϕ. Previous models have treated the case where the excited complex, (A*·Q), does not emit[16-21] ($\phi_{AQ} \cong 0$). For this case, eq 12 reduces to

$$I^0/I = (1 + k_q\tau^0[Q])(1 + K_{eq}[Q]) \quad (13)$$

The quadratic relationship between I^0/I and [Q] predicts upward curvature in Stern–Volmer plots. However, lifetime measurements are not affected by ground-state complexation, since only A emits and plots of τ^0/τ vs. [Q] would remain linear (eq 5). Thus, the combination of steady-state luminescence and lifetime measurements can provide strong evidence for a nonemitting excited ion pair.[9,21-23]

A more general analysis of steady-state luminescence involving ground-state association with quencher allows the photoexcited complex (A*·Q) to emit and undergo several possible reactions. Consider the following mechanistic possibilities:

$$(A^*\cdot Q) \xrightarrow{k_e'} (A\cdot Q) + h\nu \quad (14)$$

$$(A^*\cdot Q) \xrightarrow{k_n'} (A\cdot Q) \quad (15)$$

$$(A^*\cdot Q) \xrightarrow{k_q''} A + Q \quad (16)$$

$$(A^*\cdot Q) + Q \xrightarrow{k_q'} A + 2Q \quad (17)$$

The luminescnece quantum yield for (A*·Q) is given by

$$\phi_{AQ} = k_e'/(k_e' + k_n' + k_q'[Q] + k_q'') \quad (18)$$

Combination of the expressions for ϕ_{AQ}, $\phi_A{}^0$, and ϕ_A with eq 12 yields

$$I^0/I = (1 + K_{eq}[Q])(1 + k_q{}^0[Q])/(1 + (\tau'/\tau^0)K_{eq}[Q] \times (1 + \tau^0k_q[Q])(1 + \tau'k_q'[Q])^{-1}) \quad (19a)$$

$$\tau' = (k_e' + k_n' + k_q'')^{-1} \quad (19b)$$

(12) Kitamura, N.; Okano, S.; Tazuke, S. *Chem. Phys. Lett.* **1982**, *90*, 13.
(13) Durham, B.; Casper, J.; Nagle, J. K. Meyer, T. J. *J. Am. Chem. Soc.* **1982**, *104*, 4803.
(14) (a) Van Houten, J.; Watts, R. J. *J. Am. Chem. Soc.* **1976**, *98*, 4853; (b) *J. Inorg. Chem.* **1978**, *17*, 3381; (c) *J. Am. Chem. Soc.* **1975**, *97*, 3843.
(15) Allsopp, S. R.; Cox, A.; Kemp, T. J.; Reed, W. J. *J. Chem. Soc., Faraday Trans.* **1978**, *5*, 1275.
(16) Jamieson, M. A.; Langford, C. H.; Serpone, N.; Hersey, M. W. *J. Phys. Chem.* **1983**, *87*, 1004.
(17) Ware, W. R.; Shukla, P. R.; Sullivan, P. J.; Bremplis, R. V. *J. Chem. Phys.* **1971**, *55*, 4048.
(18) Weller, A. "Progress in Reaction Kinetics"; Porter, G., Ed.; Pergamon Press: New York, 1961; Vol. 1.
(19) Fujita, I.; Kobayashi, H. *Ber. Bunsenges. Phys. Chem.* **1978**, *83*, 655.
(20) Kano, K.; Takenoshita, F.; Ogawa, T. *J. Phys. Chem.* **1982**, *86*, 1833.
(21) Hercules, D. *Anal. Chem.* **1966**, *12*, 29A.
(22) Balzani, V.; Moggi, L.; Manfrin, M. F.; Bolletta, F. *Coord. Chem. Rev.* **1975**, *15*, 321.
(23) Ware, W. *Pure Appl. Chem.* **1975**, *41*, 635.

Two assumptions were made in deriving eq 19. First, the molar absorptivities of A and (A·Q) were assumed to be equal at the exciting wavelength, i.e., $\epsilon_A = \epsilon_{AQ}$. This was experimentally verified for the $Ru(bpy)_3^{2+}$–$S_2O_8^{2-}$ system. Absorption spectra of $Ru(bpy)_3^{2+}$ in all solvent systems employed here were essentially unchanged by the addition of $S_2O_8^{2-}$. This behavior would be expected for the formation of solvent-separated ion pairs. The second assumption made is that the radiative rate constants of free A* and the ion-paired species, (A*·Q), were equal, i.e., $k_e = k_e'$. Direct experimental verification of this assumption is not as easily accomplished. However, lifetime measurements of $Ru(bpy)_3^{2+}$ solutions were not affected appreciably by the presence of the counterions Cl^-, PF_6^-,[13] or SO_4^{2-}.[24] If the association between $Ru(bpy)_3^{2+}$ and $S_2O_8^{2-}$ is purely electrostatic (ion pairing) and does not result in a change in the inner-sphere coordination shell (e.g., by substitution or bridging to the metal center), then it is unlikely that the radiative rate constant would be perturbed.

Furthermore, the absorption and emission spectra of $Ru(bpy)_3^{2+}$ are the same in the presence and absence of $S_2O_8^{2-}$, so that the electronic structure of $Ru(bpy)_3^{2+}$ is not largely perturbed by the presence of $S_2O_8^{2-}$. No assumptions were made regarding the nonradiative pathways, which, for $Ru(bpy)_3^{2+*}$, are considerably more sensitive to solvent and temperature.[12-15]

Two limiting conditions of eq 19 can be identified:

(a) As $K_{eq}[Q] \rightarrow 0$

$$I^0/I = 1 + k_q\tau^0[Q] \tag{20a}$$

(b) When $K_{eq}[Q] \gg 1$

$$I^0/I = (1 + k_q\tau^0[Q])/(1 + (\tau'/\tau^0)(1 + k_q[Q]\tau^0)(1 + k'_q[Q]\tau')^{-1}) \tag{20b}$$

When the second term in the denominator is large compared to 1, then

$$I^0/I = (\tau^0/\tau') + k_q'\tau^0[Q] \tag{21}$$

Equation 20a is the expected SV equation when K_{eq} or [Q] is small. At large values of $K_{eq}[Q]$ (eq 21) a linear dependence of I^0/I can also occur. The overall expression for I^0/I (eq 19) predicts an initial downward curvature in SV luminescence plots at low [Q] and linear behavior at large [Q]. An independent measurement of the lifetime of A*, τ^0, in the absence of Q allows calculation of the complex excited-state lifetime τ', from the extrapolated intercept of the high [Q] linear region. Similarly, an experimental value of the bimolecular quenching rate, k_q', for the reaction between the photoexcited ion pair (A*·Q) and a second quenching molecule is obtained from the slope of the linear region. Treatment of the data in Figure 1, b and c, yields values of τ' and k_q' that are unaffected by the solution ionic strength. Values of k_q' and τ' for solutions containing various percentages of CH_3CN (by volume) are listed in Table I. The quenching rates, k_q, for solutions containing excess inert electrolyte, 0.2 M $(NH_4)_2SO_4$, as measured from the slope of the linear SV plots in Figure 3, are also listed in Table I for comparison to k_q'. Note that the values for quenching of the ion pair of $Ru(bpy)_3^{2+}$ with SO_4^{2-} (k_q) and $S_2O_8^{2-}$ (k_q') for any given solvent composition are almost the same (Table I) and decrease with increasing CH_3CN content.

Temperature Dependence. The dependence of bimolecular rate (eq 17) and ion-pair excited-state lifetime, τ', on temperature, T, was investigated by steady-state luminescence quenching measurements over the temperature range 8–45 °C. SV plots are shown in Figure 6 for solutions containing 10% CH_3CN by volume. k_q' and τ' values were calculated from the slope and extrapolated intercept as discussed above. The values of τ^0 at different temperatures were taken from data measured in pure water.[14a] These may be considered as a lower limit to the actual lifetime in 90% H_2O due to the stabilizing effect that CH_3CN has on the $Ru(bpy)_3^{2+}$ excited state (see Table I). The trends are evident; k_q' and τ' appear to be surprisingly insensitive to variations in temperature (Table II) over this limited range. The decrease in values of extrapolated intercept (Figure 6) with increasing temperature is due solely to a decrease in the τ^0 values.[13-15]

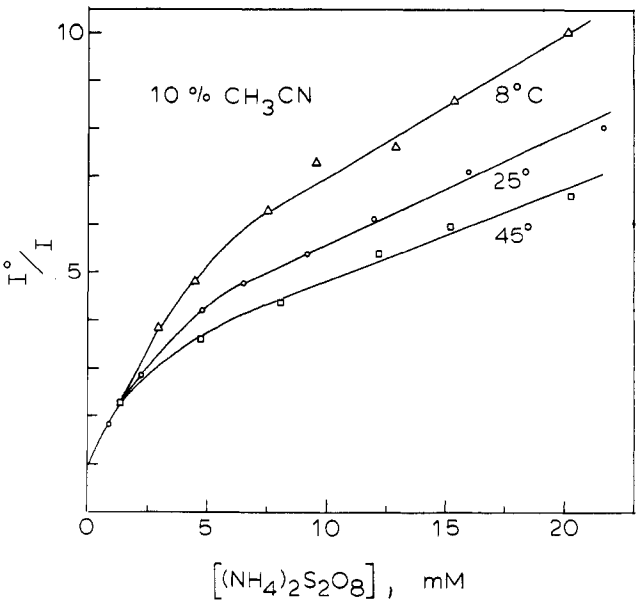

Figure 6. Effect of temperature on quenching rate. Solutions contained ca. 30 μM $Ru(bpy)_3(PF_6)_2$ and were degassed with N_2.

TABLE II: Dependence on Temperature of Kinetic Parameters of the $Ru(bpy)_3^{2+}$–$S_2O_8^{2-}$ System in 90% H_2O–10% CH_3CN

temp, °C	τ^0, μs	$10^{-8}k_q'$, M^{-1} s^{-1}	y intercept	τ', μs
8	0.71[a]	4.1	4.0	0.17
25	0.60	3.5	3.5	0.17
45	0.45	4.3	3.0	0.15

[a] Values interpolated from data in 100% H_2O of Van Houten and Watts.[14]

Ion-pair Association Constant, K_{eq}. The association constant of the ion pair $[Ru(bpy)_3^{2+}\cdot S_2O_8^{2-}]$ was determined by fitting eq 19 as a function of K_{eq} to the experimental SV plots obtained for solutions of different ionic strengths. Other variables (k_q, k_q', τ^0, and τ') used in this calculation were previously determined as discussed above from the limiting slopes and intercepts and are listed in Table I. K_{eq} values determined by this procedure are also listed in Table I and the resulting theoretical SV plots (solid lines) for 10% and 40% CH_3CN solutions are shown in Figures 1 and 2. The close agreement between experimental and calculated curves lends credence to the proposed model of ground-state ion pairing. However, considerable uncertainty exists in the values of K_{eq} determined by this procedure because of the scatter in luminescence data at low $S_2O_8^{2-}$ concentrations; in some cases, K_{eq} values within ±20% of those listed in Table I gave reasonable fits to the experimental curves. However, ion-pair association constants for the solvent system studied (0–50% CH_3CN) are within the range 5×10^2–2×10^3 M^{-1}. For comparison, the association constants calculated from the classical Fuoss–Bjerrum model of electrostatic attraction,[26] and by assuming 5-Å ionic radii, are 1×10^2 M^{-1} for H_2O and 1.6×10^5 M^{-1} for CH_3CN. The small decrease in the K_{eq} values observed in solutions containing a higher content of CH_3CN is opposite to expectations based on the Fuoss–Bjerrum model, since the lower dielectric constant of CH_3CN would be expected to increase the amount of ion pairing. This, perhaps, indicates a preferential solvation of one or both reactants by CH_3CN.

The dependence of the shape of SV plots on the ion-pair excited-state lifetime, τ', is shown in Figure 7. All other variables

(24) Values of τ^0 in the presence and absence of 0.2 M $(NH_4)_2SO_4$ were equal in solutions containing 0–50% CH_3CN by volume.

(25) Wallace, W.; Bard, A. J. *J. Phys. Chem.* **1979**, *83*, 1350.

(26) Fuoss, R. M. *J. Am. Chem. Soc.* **1958**, *80*, 5059.

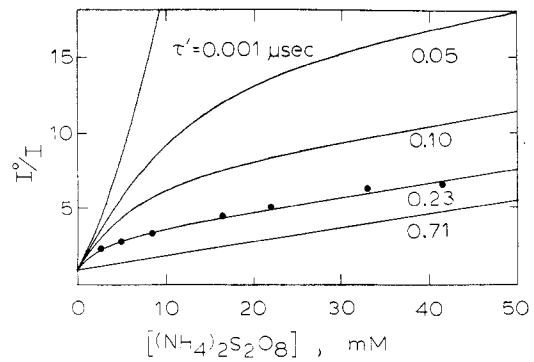

Figure 7. Theoretical Stern–Volmer plots for different ion-pair excited-state lifetimes, τ'. Curves calculated from eq 19 (see text) using K_{eq} = 950 M^{-1}, τ^0 = 0.71 μs, $k_q = k_q' = 1.3 \times 10^8$ M^{-1} s^{-1}. Experimental values of I^0/I (●) obtained in 20% CH_3CN (by volume) solution containing ca. 30 μM $Ru(bpy)_3(PF_6)_2$ and N_2 purged.

(K_{eq}, k_q', k_q, and τ^0) used in calculating the family of curves were taken from the experimental results for a 20% CH_3CN solution. For comparison, the experimental values of I^0/I vs. $[S_2O_8^{2-}]$ are also included in Figure 6. The point here is that a variety of curve shapes are obtained as the value of τ' is decreased from a value equal to τ^0 to a very small value ($\tau' \leq 10^{-9}$ s; smaller values of τ' do not result in an appreciable change in the SV plot) and that knowledge of K_{eq} alone does not suffice in predicting the shape of the SV plot. When $\tau' = \tau^0$, a linear SV plot is obtained that is indistinguishable from the expected results in the absence of ion pairing. Moderately small values of τ' yield SV plots that show downward curvature while exceptionally short lifetimes give rise to upward curvature (quadratic relationship). The latter case is that previously described by Ware and others[21-23] for a non-emitting ion pair.

Lifetimes. The coincidence of results obtained from lifetime measurements (τ^0/τ) and luminescence quenching experiments (I^0/I) is also readily understood in terms of ion-pair association. The emission–time profile predicted for solutions containing both free $Ru(bpy)_3^{2+}$ and the ion-paired species $[Ru(bpy)_3^{2+}\cdot S_2O_8^{2-}]$ is given by eq 22, where f_A and $f_{A\cdot Q}$ are the fractions of free and

$$I(t)/I(t=0) = f_A \exp\{-t(\tau^{-1} + k_q[S_2O_8^{2-}])\} + f_{AQ} \exp\{-t(\tau'^{-1} + k_q'[S_2O_8^{2-}])\} \quad (22)$$

ion-paired Ru species, respectively (eq 9 and 10). The second exponential in eq 22 is derived by considering the quenching routes for the ion pair listed in eq 14–17. The first-order quenching rate constant, k_q'', is included in τ'. Equation 22 predicts that plots of ln $I(t)$ vs. t should show two linear regions when $f_A \cong f_{AQ}$, or, in terms of the quencher concentration in the present case, at ca. 2–5 mM $S_2O_8^{2-}$. At $S_2O_8^{2-}$ concentrations above 5 mM the measured emission arises predominantly from the ion-paired species (i.e., $f_{A\cdot Q} \gg f_A$). Linear plots of ln $I(t)$ vs. t are expected in this region. Attempts to discern simultaneous emission from free and complexed Ru from lifetime measurements in the 1–5 mM $S_2O_8^{2-}$ range were unsuccessful because of a limited time window (2–3 half-lives) as well as the small differences in the luminescence decay rates of the two emitting species. For example, in purely aqueous media, the steady-state luminescence results (Table I) predict a difference of approximately 2 in the emission decay rates when $[S_2O_8^{2-}]$ = 2–5 mM.

$$(\tau'^{-1} + k_q[Q])/(\tau^{0-1} + k_q[Q]) \cong 2 \text{ in } H_2O \quad (23)$$

Smaller differences are predicted for all other solvent combinations. Thus, all emission–time profiles were fitted to a single exponential decay. Equation 22 is still quite useful in that it predicts *downward* curvature in plots of τ^0/τ vs. $[S_2O_8^{2-}]$. This is opposite to the situation of a nonemitting ion-pair complex where linear plots are expected.[21-23]

To demonstrate that the lifetime measurements yield τ^0/τ values equal to I^0/I, calculated values of τ^0/τ (based on eq 22) are plotted in Figure 2 and compared to experimental and theoretical I^0/I values and experimental τ^0/τ values. Values of $I(t)$ were calculated from eq 22 as a function of $S_2O_8^{2-}$ concentration and the kinetic parameters listed in Table I obtained from steady-state luminescence data. The theoretical $I(t)$ decay was then fitted by least squares to a single exponential decay and τ^0/τ vs. $[S_2O_8^{2-}]$ plots were constructed. Close agreement between calculated I^0/I (eq 19) and τ^0/τ (eq 22) values clearly indicates the coincidence of lifetime and steady-state data for the relatively long-lived excited complexes.

Discussion

Several questions arise concerning the fate and lifetime, τ', of the photoexcited ion pair $[Ru(bpy)_3^{2+*}\cdot S_2O_8^{2-}]$. Although the mechanistic routes listed by eq 14–17 may describe accurately reactions of the photoexcited complex, the predominant route of deactivation is not discernible from the present kinetic measurements. The difference between values of τ' and the $Ru(bpy)_3^{2+*}$ lifetime, τ^0, represents any acceleration of the nonradiative decay process inherent to the free Ru complex, in addition to new possible first-order quenching routes due to ion-pair association. Without assuming any mechanistic detail, one may express τ' as

$$1/\tau' = 1/\tau^0 + \Delta k_q' \quad (24)$$

where $\Delta k_q'$ represents the change in the $Ru(bpy)_3^{2+*}$ nonradiative rates due to ion-pair association. Values of $\Delta k_q'$ calculated from eq 24 are listed in Table I.

Previous studies concerned with determining the photooxidation rate and quantum yield of reaction 1 have employed solutions containing high concentrations of acetate (0.2 M)[2] and sulfate (2 M),[3] conditions under which $[Ru(bpy)_3^{2+}\cdot S_2O_8^{2-}]$ association is probably prevented. Thus, the high quantum yield ($\phi \sim 2$) of eq 1 determined from these studies cannot be used to infer electron transfer in the excited ion pair. Quenching via electron transfer is supported by the close resemblance of the mechanism proposed here with that suggested by Brubaker and Raman[7] for the ground-state oxidation of $Fe(bpy)_3^{2+}$ by $S_2O_8^{2-}$. Both involve the formation of the intermediate $[M(bpy)_3^{2+}\cdot S_2O_8^{2-}]$. On the basis of the redox potentials reported for $Fe(bpy)_3^{3/2+}$ and $Ru(bpy)_3^{3/2+*}$, electron transfer in the photoexcited Ru ion pair is ca. 35 kcal/mol more favorable than in the Fe intermediate. The parallel trend of bimolecular quenching rates (an electron-transfer process) with $\Delta\tau$ values (Table I) as a function of solvent composition also suggests a common deactivation mechanism, i.e., electron transfer, for both unimolecular and bimolecular quenching. In addition, quenching rates were rather insensitive to temperature in the range, 8–45 °C (Table II). Over the same temperature variation, the lifetime of $Ru(bpy)_3^{2+*}$ decreases by ~35% due to thermal equilibration of the luminescent metal-to-ligand charge-transfer state to a set of energetically higher metal nonbonding states which are known to undergo photosubstitution or rapid radiationless decay ($k \sim 10^{-13}$ s) to the ground state.[13-15] That τ' is independent of temperature suggests that ion pairing does not perturb the rate of radiationless decay through these states.

In all solvent combinations employed in these studies, the photochemical oxidation of $Ru(bpy)_3^{2+}$ by $S_2O_8^{2-}$ is sufficiently energetic to expect diffusional controlled rates. It is unlikely that the large decrease in bimolecular quenching rates, k_q, or k_q', is due to a decrease in the thermodynamic driving force of eq 1 by the addition of CH_3CN. Similarly, the differences in solvent viscosity and dielectric constant would also tend to favor faster rates in solutions containing CH_3CN. A more likely explanation of the unusual rate dependence observed here is that a kinetic barrier, due to a specific solvation of one or both reactants by CH_3CN, inhibits the rate of electron transfer. The lifetime measurements of $Ru(bpy)_3^{2+*}$ suggest a preferential solvation of this cation by CH_3CN in H_2O–CH_3CN mixed solutions. However, it is not evident how this phenomenon might affect the observed quenching rates. Further investigations of the luminescence quenching of $Ru(bpy)_3^{2+*}$ in mixed solvent systems

by one-electron outer-sphere quenchers should be of interest.

Conclusions

Luminescence quenching of $Ru(bpy)_3^{2+*}$ by $S_2O_8^{2-}$ in aqueous and mixed acetonitrile–wate solutions occurs by both unimolecular and bimolecular pathways. The nondiffusional pathway results from the ground-state association of $Ru(bpy)_3^{2+}$ with $S_2O_8^{2-}$. The lifetime of the photoexcited ion pair is shorter than $Ru(bpy)_3^{2+*}$ in all solvent combinations investigated but long enough to allow the excited complex to be quenched by a second $S_2O_8^{2-}$ as well as luminescence at the characteristic emission wavlengths of $Ru(bpy)_3^{2+*}$. An unusually strong dependence of bimolecular and unimolecular quenching rates on the solvent employed suggests that both quenching reactions occur by electron transfer and that the rate-limiting step in both mechanisms is solvent reorganization of one or both reactants.

The analysis of steady-state luminescence and lifetime measurements demonstrates that coincidence of I^0/I and τ^0/τ values is expected for the general case of ground-state ion pairing provided that the lifetime of the excited ion pair is relatively long.

Acknowledgment. This research was supported by the Army Research Office (DAAG 29-82-K-0006) and the National Science Foundation (CH7903729). The experiments and analysis of data from laser flash experiments were performed at the Center for Fast Kinetics Research (CFKR) at The University of Texas at Austin. The CFKR is supported jointly by the Biotechnology Branch of the Division of Research Resources of NIH (RR00886) and the University of Texas at Austin.

Registry No. $Ru(bpy)_3^{2+}$, 15158-62-0; $S_2O_8^{2-}$, 15092-81-6; CH_3CN, 75-05-8; H_2O, 7732-18-5; $(NH_4)_2SO_4$, 7783-20-2; $K_4Fe(CN)_6$, 13943-58-3.

A Comparative Rate Method for the Study of Unimolecular Falloff Behavior

Walter Braun, J. R. McNesby,† and Milton D. Scheer*

Center for Chemical Physics, National Bureau of Standards, Washington, D.C. 20234
(Received: June 7, 1983)

A comparative method was applied to a high-temperature fast-flow reactor to determine relative kinetic parameters for the two-channel decomposition of cyclobutanone in the falloff region. The applicability of this method to such nonthermally equilibrated systems was assessed and found to be generally useful over a wide range of conditions. The measurements could, therefore, be used as a quantitative diagnostic tool for sensing unimolecular falloff behavior in a number of heat bath gases. A simple stepladder collisional activation–deactivation model was used to determine the energy transferred per collision. The values obtained for the heat bath gases He, Ar, SiF_4, and SF_6 were 3.0, 2.0, 3.5, and 4.0 kcal/mol, respectively. These are small multiples of RT and very small fractions of the activation energy, indicating that weak collisions must be a dominant feature of reaction types represented by the decomposition of cyclobutanone.

Introduction

Energy transfer models applicable to unimolecular dissociation processes have been assessed and a considerable body of literature exists on the subject.[1-4] Still, it is not yet entirely certain how the average energy transferred per collision varies with the energy content of the decomposing molecule and the temperature of the bath gas. Although direct methods for assessing the energy transferred per collision have recently been described,[2] the usual approach, and the one which we adopt, involves (1) measuring decomposition rate constants for various pressures of the heat bath gas, (2) computing $k(E)$ vs. energy, (3) applying these energy-dependent rates to the energy level populations calculated by means of an appropriate energy transfer model, and (4) comparing the macroscopic rate constants obtained from these calculations with the experimental results.

A typical energy transfer model involves a single parameter, namely, the average energy transferred either up or down an energy ladder with constant spacing. The energy dependences of the probability of such energy transfers that have been used previously[1] are the Dirac Δ function or stepladder, the exponential function, and the Poisson and Gaussian functions. The general feature of these models are quite similar, and experimental results have not definitively distinguished between them. The comparative experimental method of evaluating kinetic parameters has been successfully applied at high pressures to fully thermalized unimolecular systems in single-pulse shock tubes by Tsang.[5] We have adapted his method to a study of the kinetics of flowing reactive systems at much lower pressures. The method compares the ratio of decomposition rates of two simultaneously occurring reactions and is insensitive to temperature inhomogeneities (see Appendix). The measurements that we will describe complement those made at much lower pressures by the so-called "very low-pressure pyrolysis" (VLPP) method.[6-8] The VLPP measurements are taken with decomposition occurring where the activated reactant energies are very close to E_0, the threshold energy, while at higher pressures progressively higher energy levels become involved. The measurements described here for heated flow systems can also be compared with infrared laser heating.[9-13]

† Chemistry Department, University of Maryland, College Park, MD 20742.

(1) D. C. Tardy and B. S. Rabinovitch, *J. Chem. Phys.* **45**, 3720 (1966); D. C. Tardy and B. S. Rabinovitch, *Chem. Rev.*, **77**, 369 (1977).
(2) J. R. Barker, M. J. Rossi, and J. R. Pladziewicz, Abstracts of papers presented at the "7th International Symposium on Gas Kinetic", University of Gottingen, Gottingen, Germany, 1982; H. Hippler, J. Troe, and H. J. Wendelken, *Ibid.*
(3) R. C. Bhattacharjee and W. Forst, *Chem. Phys.*, **30**, 217 (1978); **37**, 343 (1979).
(4) N. Snider, *J. Chem. Phys.*, **78**, 6030 (1983).
(5) See, for example, (a) W. Tsang, *Int. J. Chem. Kinet.*, **10**, 599 (1978); (b) W. Tsang, in "Shock Waves in Chemistry", Lifshitz, Ed., Marcel Dekker, New York, 1981, Chapter 2.
(6) D. M. Golden, G. N. Spokes, and S. W. Benson, *Angew. Chem., Int. Ed., Engl.*, **12**, 534 (1973).
(7) R. B. Gilbert and K. D. King, *Chem. Phys.*, **49**, 367 (1980).
(8) K. D. King, T. T. Nguyen, and R. G. Gilbert, *Chem. Phys.*, **61**, 221 (1981).
(9) W. Braun, M. J. Kurylo, and A. Kaldor, *Chem. Phys. Lett.*, **28**, 440 (1974).
(10) W. Shaub and H. S. Bauer, *Int. J. Chem. Kinet.*, **7**, 509 (1975).
(11) V. Starov, N. Selamogh, and C. Steel, *J. Am. Chem. Soc.*, **103**, 7276 (1981).
(12) D. F. McMillan, K. E. Lewis, G. P. Smith, and D. M. Golden, *J. Phys. Chem.*, **86**, 709 (1982).
(13) M. D. Scheer, J. R. McNesby, and W. Braun, following paper in this issue.

0022-3654/84/2088-1846$01.50/0